

Figure 4 shows the expected event numbers due the pair production process. More than  $10^9$  events would be expected over a large mass range for  $\epsilon \approx 0.03$ . For  $\epsilon > 0.1$  the sensitivity quickly drops as the dark photons start to be absorbed in the iron absorber in front of the detector as normal photons do. For  $\epsilon < 10^{-4}$  the combined production and interaction probability, which scales as  $\epsilon^4$  in this range, becomes too small to produce any detectable signal. The narrowing of the contour for  $0.01 \text{ eV} < m_{\gamma'} < 10 \text{ eV}$  is due to the oscillation term of Eq. (31).

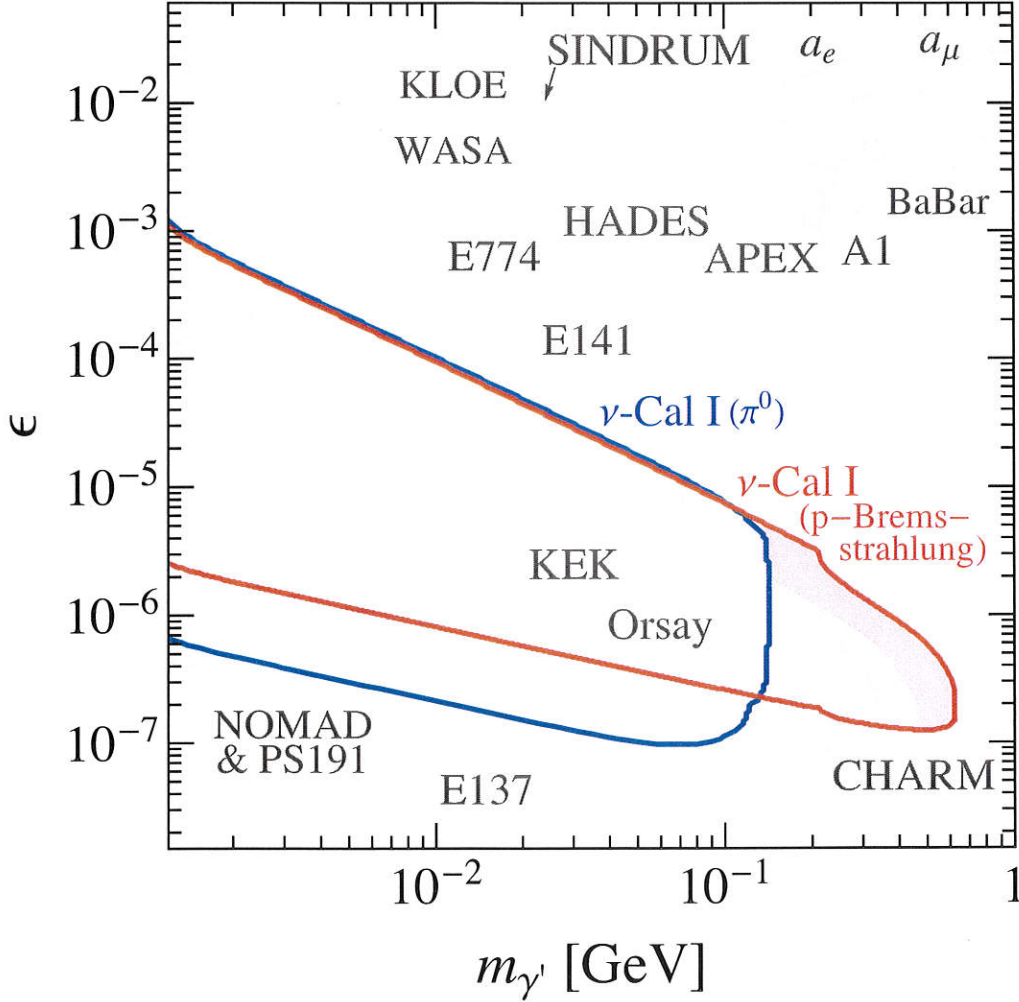


Figure 5: Comparison of the present exclusion bounds (red area and lines) with other exclusion limits (grey area and lines) derived from data on the anomalous magnetic moments of the electron and muon [14],  $\Upsilon(3S)$  decays [15], Belle [16],  $J/\psi$ -decays [17],  $K$ -decays [18], KLOE-2 [19], A1 [20], APEX [21], HADES [22], E774 [23], E141 [24], E137 [25, 26], Orsay [27], KEK [28], NOMAD and PS191 [29], CHARM [30], SINDRUM [31], WASA [32] and  $\nu$ -CAL I for  $\pi_0$ -decay [3] (blue line).<sup>6</sup>

Using the pair production channel, the present analysis is sensitive to  $\gamma'$  particles in the approximate range of  $5 \cdot 10^{-5} < \epsilon < 10^{-1}$  and  $0.1 \text{ eV} < m_{\gamma'} < 1 \text{ MeV}$ . Confronting this with a summary exclusion plot as Figure 4 of [72], this range has already been excluded by different methods such as solar lifetime considerations and precision measurements of the Rydberg constant. However, the value of the present analysis consists in using a direct detection method which is largely model independent.

<sup>6</sup>We thank S. Andreas for designing this graph. The exclusion curves for the electron-beam dump have been recalculated in [40] and are shown here. Note a difference to [12] in case of E137.

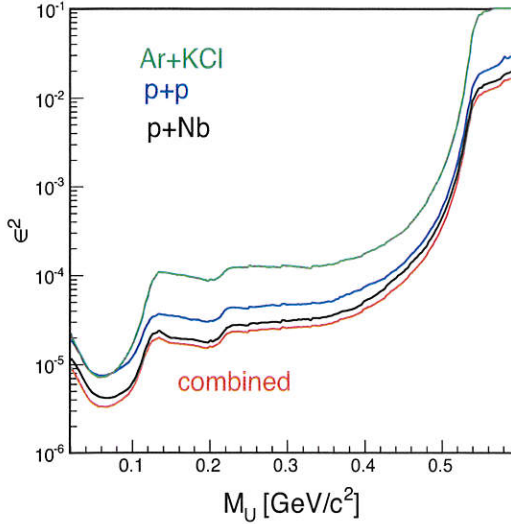


Fig. 4. (Color online) Exclusion plot at 90% CL on  $\epsilon^2$  as function of  $M_U$  from the analyses of HADES in the reactions  $p(3.5 \text{ GeV}) + \text{Nb}$ , as well as  $\text{Ar}(1.756 \text{ GeV}/u) + \text{KCl}$ . Also shown is the combined UL computed with Eq. (8).

median while staying indeed within the expected

corridors with roughly the expected rate.

The inserts in Fig. 3 show, as a function of mass, the pair efficiency and acceptance correction factor,  $eff \times acc$ , obtained from detailed simulations. After having corrected the median UL for this factor, Eq. (7) was used to compute a corresponding upper limit  $UL(\epsilon^2)$  on the relative coupling strength  $\epsilon^2$  of a hypothetical dark vector boson. Figure 4 shows the  $UL(\epsilon^2)$  as a function of  $M_U$  obtained from the three data sets separately. Evidently, the p+Nb data provide the strongest constraint. However, as the three data sets are of comparable statistical quality and result hence in upper limits of similar magnitude, it is natural to join them into a combined upper limit [46]. Since all experiments having been executed under very similar conditions, we use the following statistics-driven ansatz:

$$UL_{(1+2+3)} = \sqrt{(UL_{(1)}^{-2} + UL_{(2)}^{-2} + UL_{(3)}^{-2})^{-1}}. \quad (8)$$

The combined upper limit  $UL_{(1+2+3)}$  is overall about 10 to 20% lower than the p+Nb value taken alone. This is indeed expected from the moderate increase in pair statistics achieved by cumulating the data from all experiments and is consistent with a  $UL \propto 1/\sqrt{N}$  behavior.

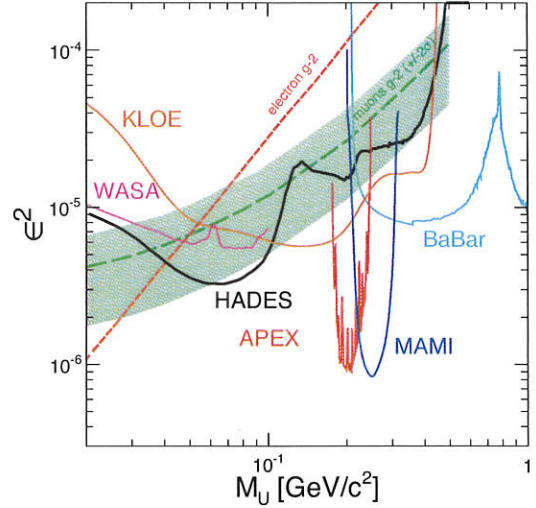


Fig. 5. (Color online) The 90% CL upper limit on  $\epsilon^2$  versus the  $U$ -boson mass obtained from the combined analysis of HADES data (solid black curve). This result is compared with existing limits from the MAMI/A1, APEX, BaBar, WASA, and KLOE-2 experiments, as well as with the  $g-2$  constraints (see the text for citations).

Finally, in Fig. 5 we show the HADES result together with a compilation of limits from the searches conducted by BaBar [47,18,20], KLOE-2 [26,27], APEX [23], WASA at COSY [25], and A1 at MAMI [22]. At low masses ( $M_U < 0.1 \text{ GeV}/c^2$ ) we clearly improve on the recent result obtained by WASA [25], excluding now to a large degree the parameter range allowed by the muon  $g-2$  anomaly (prediction with  $2\sigma$  interval is shown on the Fig. 5). At higher masses, the sensitivity of our search is compatible with, albeit somewhat lower than the combined KLOE-2 analysis of  $\phi$  decays. Our data probe, however, the  $U$ -boson coupling in  $\eta$  decays and add hence complementary information. At masses above the  $\eta$  mass, the inclusive dilepton spectrum is fed by  $\Delta$  (and to some extent heavier baryon resonance) decays which offer only small sensitivity, partly due to the small electromagnetic branching ratio ( $BR_{N\gamma} \simeq 10^{-3} - 10^{-2}$ ) and partly due to the decreasing  $BR_{U \rightarrow ee}$  at high  $M_U$ .

## 5. UL on the rare decay $\eta \rightarrow e^+e^-$

The direct decay of the  $\eta$  meson into a lepton pair ( $e^+e^-$  or  $\mu^+\mu^-$ ) can only proceed through a 2-photon intermediate state. The  $e^+e^-$  decay is fur-